

# Small- and large- $x$ nucleon spin structure from a global QCD analysis of polarized Parton Distribution Functions

E. R. Nocera<sup>a,\*</sup>

<sup>a</sup>*Dipartimento di Fisica, Università di Genova and INFN, Sezione di Genova,  
Via Dodecaneso, 33 I-20146 Genova, Italy*

---

## Abstract

I investigate the behavior of spin-dependent parton distribution functions in the regions of small and large momentum fractions  $x$ . I present a systematic comparison between predictions for relevant observables obtained with various models of nucleon spin structure and a recent global analysis of spin-dependent distributions, NNPDFpol1.1. Together with its unpolarized counterpart, NNPDF2.3, they form a mutually consistent set of parton distributions. Because they include most of the available experimental information, and are determined with a minimally biased methodology, these are especially suited for such a study. I show how NNPDFpol1.1 can discriminate between different theoretical models, even though NNPDF uncertainties remain large near the endpoints  $x \rightarrow 0$  and  $x \rightarrow 1$ , due to the lack of experimental information. I discuss how our knowledge of nucleon spin structure may be improved at small  $x$  by future measurements at an Electron-Ion Collider, and at large  $x$  by recent measurements at Jefferson Lab, also in view of its 12 GeV upgrade.

**Keywords:** parton distribution functions (PDFs), polarized nucleon structure, Regge theory, hadron models

**PACS:** 12.39.-x, 12.40.Nn, 13.88.+e

---

*Introduction.* The behavior of spin-dependent, or polarized, Parton Distribution Functions (PDFs) at small and large momentum fractions  $x$  has been recognized for a long time to be of particular physical interest [1, 2]. On the one hand, the small- $x$  region is pivotal for revealing new aspects of the nucleon picture depicted by Quantum Chromodynamics (QCD), related, for instance, to PDF evolution. On the other hand, the large- $x$  region is definitive of hadrons: indeed, all Poincaré-invariant properties of a hadron, like flavor content and total spin, are determined by valence quark PDFs in the region  $x \gtrsim 0.2$ , where they are expected to dominate. Above all, an accurate knowledge of polarized PDFs over a broad range of  $x$  values is required to reduce the uncertainty with which the first moments of polarized distributions and structure functions can be determined. This is relevant for testing various sum rules [3–6] and potential SU(3) flavor-symmetry breaking [7], and finally for assessing quark and gluon contributions to the nucleon spin.

Several recent studies [8–16] have presented a determination of polarized PDFs, along with an estimate of their uncertainties. These parton sets differ in the choice of data sets, details of the QCD analysis (such as the treatment of heavy quarks or higher-twist corrections) and the methodology used to determine PDFs, including the form of PDF parameterization and error propagation (for details, see *e.g.* Chap. 3 in Ref. [17]).

Despite remarkable experimental efforts, the kinematic coverage of the available data sets to be included in global analyses is still rather limited. Specifically, the accessed range of parton momentum fractions is roughly  $10^{-3} \lesssim x \lesssim 0.5$ : thus, a determination of polarized PDFs outside this region would be very much prone to the functional form used for extrapolation.

Various models have been developed for predicting the polarized PDF behavior at small and large  $x$ . Computations based on different models often lead to rather different expectations for some polarized observables. A way to discriminate among models, and eventually test their validity, is to compare predictions for such observables, obtained within either a given model or a reference parton set. The latter should be determined from a global QCD analysis of experimental data.

The goal of this paper is to present such a comparison in a systematic way, separately for small- and large- $x$  regions. I will also discuss how our knowledge of nucleon spin structure may be improved, respectively at small and large  $x$ , by future measurements at a high-energy polarized Electron-Ion Collider (EIC) [18], and by recent measurements at Jefferson Lab (JLAB), also in view of its 12 GeV upgrade [19].

In order for this study to be effective, the choice of the reference PDF set is crucial. On the one hand, it is highly desirable that most of the available experimental information is included in it, so that the unknown extrapolation region is reduced as much as possible. On the other hand, it is fundamental that a minimal set of theoretical assump-

---

\*Corresponding author

Email address: emanuele.nocera@edu.unige.it (E. R. Nocera)

tions and a procedure which allows for a faithful estimate of PDF uncertainties are used.

Among all PDF sets available in the literature, the NNPDF parton sets are those which best fulfill the aforementioned requirements (and possibly the only). Hence, these will be used in this study: specifically, NNPDFpo11.1 [16] for polarized PDFs and NNPDF2.3 [20] for the unpolarized, whenever also these will be needed.

Concerning the experimental information included in these parton sets, a large amount of high-precision Hadron Electron Ring Accelerator (HERA) and Large Hadron Collider (LHC) data are taken into account in NNPDF2.3, while polarized hadron collider data sets, specifically jet and  $W$ -boson production provided by the Relativistic Heavy Ion Collider (RHIC), are used in NNPDFpo11.1. Some of these data are missing in other global unpolarized/polarized analyses so far. In the unpolarized case, only a subset of LHC data are included in recent PDF determinations [21]. In the polarized case,  $W$ -boson production data are included only in NNPDFpo11.1, and jet production data are included only in NNPDFpo11.1 and in the determination of Ref. [15]. Other recent analyses are based on inclusive Deep-Inelastic Scattering (DIS) data solely [8, 11, 12, 14], or on inclusive and semi-inclusive DIS (SIDIS) data [9, 10, 13].<sup>1</sup> SIDIS data sets are not included in NNPDFpo11.1. However, these bring in information mostly on quark-antiquark separation at medium- $x$  values, and they are expected to be of limited importance in the small- and large- $x$  regimes, where, in addition, one expects respectively  $\Delta q \sim \Delta \bar{q}$  and  $\Delta q \gg \Delta \bar{q}$ . Then, NNPDF parton sets include all the experimental information relevant for this study.

Concerning the procedure used for PDF determination, NNPDF parton sets are based on a methodology which uses a Monte Carlo sampling and representation of PDFs, and a parameterization of PDFs based on neural networks with a redundant number of free parameters. Both these features allow for providing a PDF set in which the *procedural* uncertainty (due to the methodology used to determine PDFs from data) is reduced as much as possible. Most importantly, thanks to the neural network parameterization, the PDF behavior at small and large  $x$  can deviate from the powerlike functional form usually assumed in other PDF parameterizations. All NNPDF parton sets, both unpolarized and polarized, are determined within this methodology in a mutually consistent way.

*Small- $x$  behavior.* What the behavior of polarized PDFs should be at  $x \rightarrow 0$  is presently not well understood. Nevertheless, several models attempt to provide an estimate of the polarized, neutral-current, virtual-photon, DIS structure function  $g_1$  at small- $x$  values. Arguments based on

the dominance of known Regge poles [22] lead to the expectation

$$g_1(x) \xrightarrow{x \sim 0} x^{-\lambda} , \quad (1)$$

where  $\lambda$  is the intercept of the  $a_1(1260)$  meson Regge trajectory in the isovector channel and the  $f_1(1285)$  meson trajectory in the isoscalar channel. Roughly, this leads to [23]

$$-0.4 \leq \lambda_{a_1} \approx \lambda_{f_1} \leq -0.18 . \quad (2)$$

A model of the pomeron based on nonperturbative gluon exchange [24] gives the singular behavior

$$g_1(x) \xrightarrow{x \sim 0} A(-2 \ln x - 1) , \quad (3)$$

while it has also been argued [25] that it is possible to induce the extremely singular behavior

$$g_1(x) \xrightarrow{x \sim 0} \frac{B}{x \ln^2 x} , \quad (4)$$

where  $A$  and  $B$  are normalization coefficients determined from a fit to experimental data.

Regge theory is expected to be valid only at low  $Q^2$  and a behavior of the form (1) is unstable under DGLAP evolution [26–28]. Indeed, as  $Q^2$  increases, contributions proportional to  $\ln(1/x)$  enter the evolution equations via the splitting functions, which, in the polarized case, all contain singularities [29]. Small- $x$  logarithms are included via DGLAP evolution up to NLO accuracy in global QCD analyses of polarized PDFs. However, polarized splitting functions are further enhanced at N<sup>n</sup>LO by *double* logarithms of the form  $\alpha_s^n \ln^{2n-1} x$ , which correspond to the ladder diagrams with quark and gluon exchanges along the ladder. Calculations summing up these contributions, either with non-running [30, 31] or running [32] values of the strong coupling  $\alpha_s$ , found that the singlet flavor combination of proton and neutron structure functions,  $g_1^p + g_1^n$ , should diverge more rapidly than the nonsinglet combination,  $g_1^p - g_1^n$ , as  $x$  goes to zero, *i.e.*

$$|g_1^p + g_1^n| - |g_1^p - g_1^n| \geq 0 , \quad x \rightarrow 0 . \quad (5)$$

The next-to-next-to-leading order (NNLO) corrections to the polarized splitting functions have been computed very recently [33]: these are found to be small and unproblematic down to at least  $x \sim 10^{-4}$ .

Finally, coherence arguments [34, 35] suggest that, at a typical nucleon scale, the polarized gluon distribution  $\Delta g(x)$  should be related to its unpolarized counterpart,  $g(x)$ , according to

$$\frac{\Delta g(x)}{g(x)} \xrightarrow{x \sim 0} 2x . \quad (6)$$

In order to test the validity of expectations (1-6), corresponding predictions are made using NNPDFpo11.1 [16] and NNPDF2.3 [20] parton sets. No model assumptions were imposed for constraining the small- $x$  behavior of these PDFs,

<sup>1</sup>Note that pion production data from RHIC, not included in NNPDFpo11.1, are also taken into account in the determinations of Refs. [9, 15]. It was argued in Ref. [16] that these data may have a limited impact though.

except the requirement that polarized PDFs must be integrable, *i.e.* they have finite first moments.

In order to study the potential impact of future measurements at an EIC, the NNPDFpolEIC-B [36] parton set will be used too. This was determined from a fit to the inclusive DIS data in NNPDFpol1.1, supplemented with simulated inclusive DIS pseudodata at a future EIC down to  $x \sim 10^{-5}$ . These pseudodata were generated assuming that the *true* underlying set of PDFs is that in Ref. [9], even though the behavior of polarized PDFs at such small- $x$  values is not known. Hence, the NNPDFpolEIC-B parton set does encode information on the potential reduction of PDF uncertainties from future DIS measurements at an EIC, but definitely does not encode additional information on the small- $x$  behavior of polarized PDFs.

The impact of future measurements at an EIC was previously addressed also in Ref. [37], where projected neutral-current DIS and SIDIS artificial data were added to the DSSV polarized PDF set of Ref. [9]. In comparison to the NNPDFpolEIC-B determination, pseudodata were generated assuming the same underlying set of PDFs, but they were then included in a global QCD analysis using a substantially different fitting methodology. For this reason, since the NNPDF [36] and the DSSV [37] studies found similar PDF uncertainties, error bands can be reasonably trusted in the NNPDFpolEIC-B parton set. Only real data will determine what should be the central value instead.

In Fig. 1 (left panel), the spin-dependent structure function of the proton,  $g_1$ , is shown as a function of  $x$  at  $Q^2 = 4 \text{ GeV}^2$ , together with available experimental data from SMC [38], E143 [39], COMPASS [40] and HERMES [41] experiments, and model expectations, Eqs. (1-4). In Fig. 1 (right panel), the quantity defined in Eq. (5) is displayed at  $Q^2 = 4 \text{ GeV}^2$ . In Fig. 2 (left panel), the ratio of polarized to unpolarized gluon PDFs,  $\Delta g/g$ , is plotted in the small- $x$  region at  $Q^2 = 4 \text{ GeV}^2$ . In Fig. 3, the small- $x$  effective exponents

$$\alpha_q(x, Q^2) = -\frac{\partial \ln |q(x, Q^2)|}{\partial \ln x} \quad (7)$$

are displayed as a function of  $x$  at  $Q^2 = 4 \text{ GeV}^2$  for unpolarized NNPDF2.3 and polarized NNPDFpol1.1 PDFs,  $q = u, \bar{u}, d, \bar{d}, \bar{s}, g$  and  $q = \Delta u, \Delta \bar{u}, \Delta d, \Delta \bar{d}, \Delta \bar{s}, \Delta g$  respectively. The corresponding values at  $x = 10^{-5}$  are reported in Tab. 1. All predictions based on NNPDF parton sets are obtained at NLO QCD accuracy, and corresponding uncertainties are nominal one- $\sigma$  bands.

Inspection of Figs. 1-2-3 and Tab. 1 allows for drawing the following conclusions.

- Because of the lack of experimental information, the prediction for the small- $x$  behavior of the proton structure  $g_1^p$  obtained from the NNPDFpol1.1 parton set is largely uncertain. As a consequence, it does not allow for discriminating between powerlike Regge expectations, Eqs. (1-2), and other behaviors,

Eqs. (3-4). A substantial reduction of the uncertainty on  $g_1^p$ , up to one order of magnitude, is expected to be provided by a future EIC, as suggested by the corresponding prediction obtained using the NNPDFpolEIC-B parton set. In this case, one will be able to discriminate between expectations (1-5).

- The NNPDFpol1.1 prediction does not support the expectation (5) at moderately small- $x$  values,  $x \gtrsim 10^{-3}$ . This conclusion is consistent with the results reported by the SMC experiment on singlet and non-singlet structure function combinations,  $g_1^p + g_1^n$  and  $g_1^p - g_1^n$  [38]. It was suggested in Ref. [44] that the discrepancy observed between Eq. (5) and SMC data (and hence the NNPDFpol1.1 prediction) may be explained by significant corrections due to sub-leading terms, which may eventually alter Eq. (5). If anything, the expectation (5) is fulfilled by the corresponding prediction obtained with NNPDFpol1.1 at  $x \lesssim 10^{-3}$ . However, the latter may not be reliable, because of the complete lack of data. Also, all double-logarithmic contributions are neglected in the DGLAP evolution of the structure function  $g_1$ : these contributions may become important in the small- $x$  region and may be resummed to all orders in  $\alpha_s$  [32].
- In order to get a feeling of the potential reduction of the uncertainty attained at a future EIC, the prediction for Eq. (5) obtained using the NNPDFpolEIC-B parton set is also shown in the right panel of Fig. 1. However, in the NNPDFpolEIC-B fit only pseudodata for an EIC with a proton beam were included; in order to properly address expectation (5), it would be necessary to measure the neutron structure function  $g_1^n$  in addition. This could be done with a beam of polarized  $^3\text{He}$ . Such a measurement will also be required to improve the accuracy with which the Bjorken sum rule [3] can be checked in the deeply small- $x$  region. Indeed, in Ref. [12] it was pointed out that a largely uncertain, and potentially substantial, contribution to it may arise in this region.
- The expectation for the ratio of polarized to unpolarized gluon distribution, Eq. (6), is consistent with the prediction obtained using the NNPDFpol1.1 parton set. However, this quantity remains largely uncertain at  $x \lesssim 4 \cdot 10^{-3}$ , because of the lack of experimental data in this region. The potential reduction of this uncertainty, due to a future EIC, can be appreciated by comparing the predictions obtained using either the NNPDFpol1.1 or the NNPDFpolEIC-B parton sets. At  $x \sim 10^{-4}$ , the uncertainty estimate from the latter may be smaller than that from the former up to one order of magnitude.
- The effective exponents  $\alpha_q$ , Eq. (7), estimate the powerlike behavior of PDFs at sufficiently small- $x$  values, where the latter can be approximated as  $q \sim$

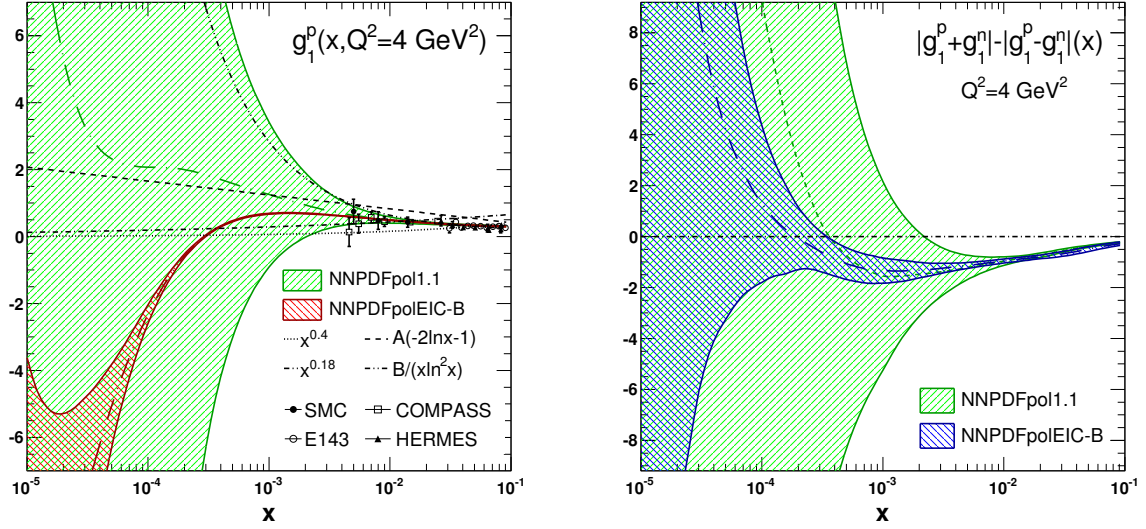


Figure 1: (Left panel). The spin-dependent structure function of the proton,  $g_1^p$ , as a function of  $x$  at  $Q^2 = 4 \text{ GeV}^2$ . Predictions are obtained using PDFs from NNPDFpol1.1 [16] and NNPDFpolEIC-B [36] parton sets. Experimental data at small  $x$  from SMC [38], E143 [39], COMPASS [40] and HERMES [41], and theoretical expectations, Eqs. (1-4), are also shown. The values of the normalization coefficients  $A$  and  $B$  entering predictions (2)-(3) are taken respectively from Ref. [24] and Ref. [25]:  $A = 0.09$  and  $B = 0.135$ . (Right panel). The prediction, Eq. (5), at  $Q^2 = 4 \text{ GeV}^2$  obtained using the same PDF sets as in left panel. Note that Eq. (5) is fulfilled whenever curves are positive.

PDF set	Ref.	$u$	$\bar{u}$	$d$	$\bar{d}$	$\bar{s}$	$g$
NNPDF2.3	[20]	$1.22 \pm 0.36$	$1.23 \pm 0.36$	$1.22 \pm 0.36$	$1.23 \pm 0.36$	$1.31 \pm 0.25$	$1.49 \pm 0.52$
NNPDFpol1.1	[16]	$0.92 \pm 1.08$	$0.61 \pm 0.39$	$0.63 \pm 1.03$	$0.64 \pm 0.28$	$0.81 \pm 0.80$	$0.73 \pm 0.15$

Table 1: The values of small- $x$  effective exponents, Eq. (7), at  $x = 10^{-5}$  and  $Q^2 = 4 \text{ GeV}^2$ .

$x^{-\alpha_q}$ ;  $q$  denotes either unpolarized or polarized distributions, respectively  $q = u, \bar{u}, d, \bar{d}, s, \bar{s}, g$  or  $q = \Delta u, \Delta \bar{u}, \Delta d, \Delta \bar{d}, \Delta s, \Delta \bar{s}, \Delta g$ . Note that the definition (7) differs from that given by Eq. (67) in Ref. [12], in that the derivative with respect to  $x$  of both the numerator and the denominator is used. In comparison to the latter definition, subasymptotic corrections, which may become negligible only at extremely small values of  $x$  (and hence may contribute to the effective exponents significantly), are taken into account in the former definition. For this reason Eq. (7) is used in the present study. Similar arguments also hold at large  $x$ , hence the definition of the asymptotic exponents given by Eq.(68) in Ref. [12] will be consistently supplemented with the derivative of both the numerator and the denominator, see Eq. (8) below.

- Results in Tab. 1 and in Fig. 3 show that the behavior of effective exponents for unpolarized PDFs is almost insensitive to the quark/antiquark flavor: indeed, the effective exponents for  $u, \bar{u}, d, \bar{d}$  distributions are very similar among each others. This conclusion does not hold for polarized PDFs, whose effective exponents show a less regular behavior than

their unpolarized counterparts.

- At sufficiently small values of  $x$ , the effective exponents are expected to enter an asymptotic regime, *i.e.* to become constant. Such a behavior is clearly visible for the polarized gluon distribution at  $x \lesssim 10^{-4}$ . For quark and antiquark PDFs, the effective exponents are still slightly varying at  $x \sim 10^{-5}$ , thus suggesting that the asymptotic regime is reached at smaller values of  $x$ . In the polarized case, experimental data used to constrain PDFs are located at  $x \gtrsim 10^{-3}$ : because below this value the stability of the effective exponents is not reached, one should conclude that the effect of data on extrapolation is rather mild.

*Large- $x$  behavior.* The behavior of polarized PDFs at  $x \rightarrow 1$  is predicted by a number of different theoretical models. To first approximation, the constituent quarks in the nucleon are described by SU(6) wave functions with zero orbital angular momentum [45]. In fact, SU(6) symmetry is known to be broken [46] and, depending on the details of SU(6)-breaking mechanisms, different behaviors of valence quarks may arise. For instance, the Relativistic Constituent Quark Model (RCQM) assumes that SU(6) sym-

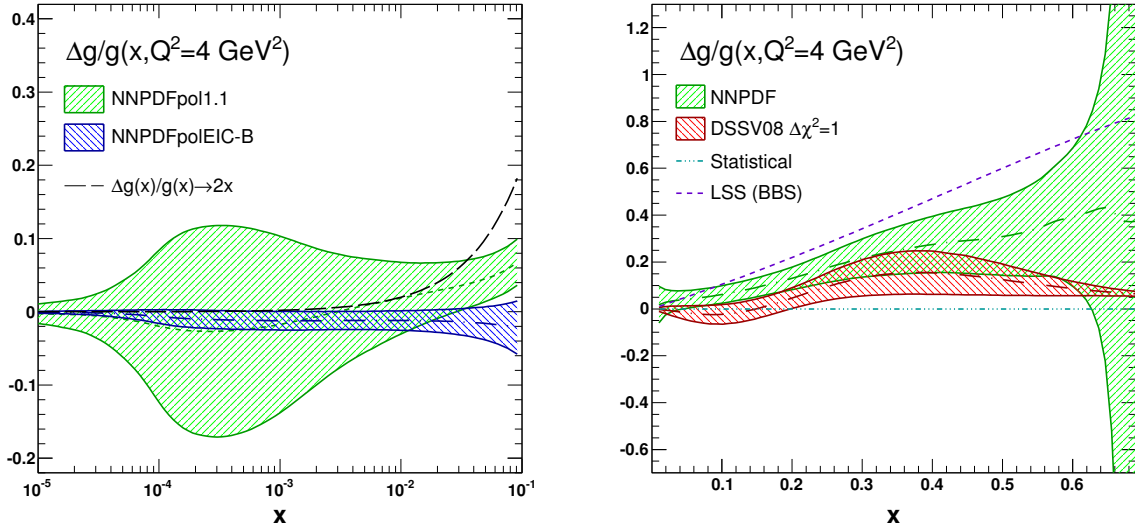


Figure 2: The ratio of polarized to unpolarized gluon PDFs,  $\Delta g/g$ , as a function of  $x$  at  $Q^2 = 4 \text{ GeV}^2$  both in the small- (left panel) and large- $x$  (right panel) regions. Predictions are obtained using NLO polarized NNPDFpol1.1 [16] and unpolarized NNPDF2.3 [20] parton sets. Predictions obtained using polarized NNPDFpolEIC-B [36] parton set instead of NNPDFpol1.1 are also displayed in the small- $x$  region. Expectations from both Eq. (6) and statistical [42] and LSS(BBS) [43] parameterizations, available in the small- and large- $x$  regions respectively, are shown for comparison.

metry is broken via a color hyperfine interaction between quarks [47]. This leads to a non-zero quark orbital angular momentum, and a consequent reduction of the valence quark contributions to the nucleon spin at large  $x$ . Different mechanisms of SU(6) breaking, consistent with duality, were also included in Quark-Hadron Duality (QHD) models [48].

Statistical models also predict the behavior of polarized PDFs at large  $x$ . They treat the nucleon as a gas of massless partons at thermal equilibrium, using both chirality and DIS data to constrain the thermodynamic potential of each parton species [42]. Both scalar and axial diquark channels have been included in a modified Nambu-Jona-Lasinio (NJL) model [49].

An approach to nucleon structure based on Dyson-Schwinger Equations (DSE), in which it is described according to the relevant Poincaré-covariant Faddeev equation, has been studied recently [50], assuming the simplification that the sum of soft, dynamic, non-pointlike diquark correlations approximates the quark-quark scattering matrix. Further expectations are provided by chiral soliton [51], instanton [52] and bag [53] models.

In leading-order (LO) perturbative QCD (pQCD), at large  $x$  and large  $Q^2$ , the valence quark orbital angular momentum may be assumed to be negligible, thus leading to hadron helicity conservation [54]. Parameterizations of the world DIS data have been made with and without this assumption. Specifically, this is included in the LSS(BBS) parton determination [43], while Fock states with nonzero quark orbital angular momentum are considered in a parameterization by Avakian *et al.* [55].

In Tab. 2 model expectations for various ratios of polarized/unpolarized PDFs and spin-dependent neutron and proton virtual photoabsorption asymmetries,  $A_1^n$  and  $A_1^p$ , at  $x \rightarrow 1$  are collected. Specifically, results for SU(6) [45], RCQM [47], QHD with two different SU(6)-breaking mechanisms [48], NJL [49], DSE *realistic* and *contact* [50] models, and the LO pQCD prediction assuming zero orbital angular momentum [54] are reported. The corresponding NNPDF predictions are also shown at  $Q^2 = 4 \text{ GeV}^2$  for different values of  $x$ .

In Fig. 2 (right panel) and Fig. 4 respectively, the ratios of polarized to unpolarized gluon distributions,  $\Delta g/g$ , and total  $u$  and  $d$  quark combinations,  $\Delta q^+/q^+ = (\Delta q + \Delta \bar{q})/(q + \bar{q})$ ,  $q = u, d$ , are displayed as a function of  $x$  at  $Q^2 = 4 \text{ GeV}^2$ . Expectations from statistical [42], NJL [49] and QHD [48] (with two different SU(6)-breaking mechanisms) models and from LSS(BBS) [43] and Avakian *et al.* [55] parameterizations are shown. Notice that not all of them are available for the gluon. The curve labeled DSSV08 is obtained using the polarized DSSV08 [9] and the unpolarized MRST [56] parton sets (the latter was used for reference in [9]). The uncertainty is the Hessian uncertainty computed assuming  $\Delta\chi^2 = 1$ . This choice may lead to somewhat underestimated uncertainties: it is well known that, in global fits based on Hessian methodology, a tolerance  $\Delta\chi^2 = T > 1$  is needed for faithful uncertainty estimation. Indeed, in Ref. [9], uncertainty estimates obtained from the Lagrange multiplier method with  $\Delta\chi^2/\chi^2 = 2\%$  (roughly corresponding to  $T \sim 8$ ) were recommended to be more reliable. In this case, the uncertainties of the DSSV08 curves would be larger than those shown in Figs. 2-4 by a

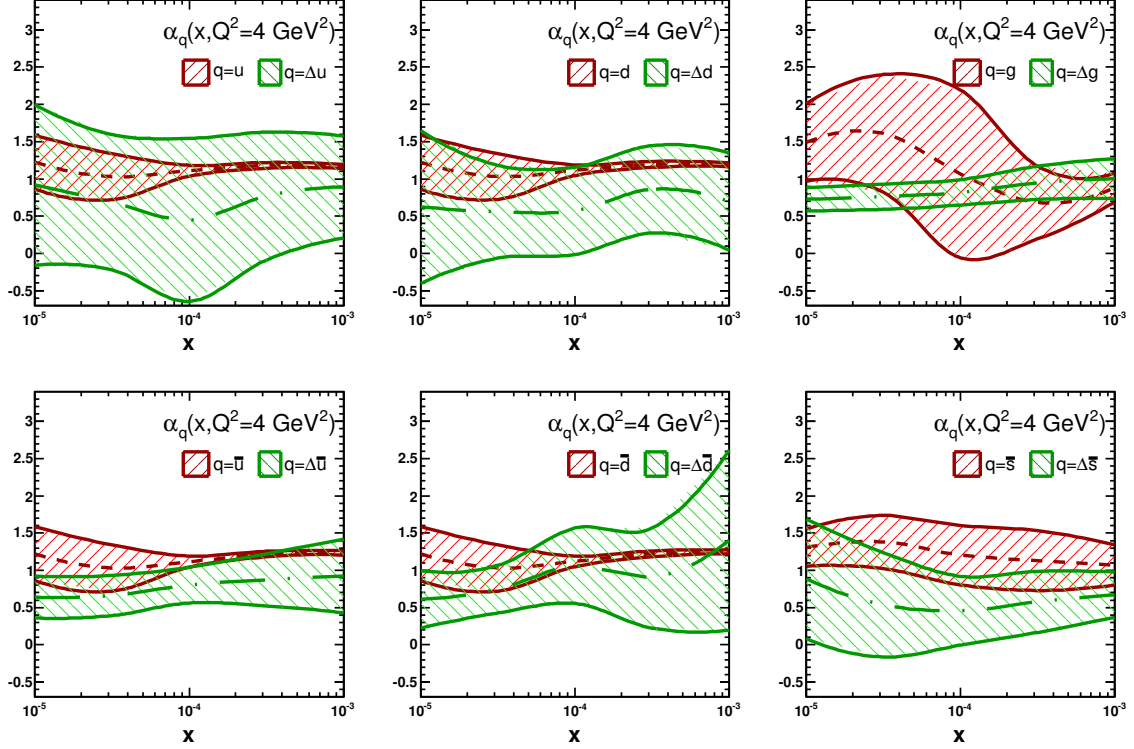


Figure 3: Small- $x$  effective exponents, Eq. (7), at  $Q^2 = 4 \text{ GeV}^2$  as a function of  $x$ .

factor  $\sqrt{T}$ .

In Fig. 5, the neutron and proton spin-dependent virtual photoabsorption asymmetries,  $A_1^p$  and  $A_1^n$ , are displayed as a function of  $x$  at  $Q^2 = 4 \text{ GeV}^2$ . When available, model expectations are shown as in Fig. 4 and supplemented with the RCQM prediction [47].

In Fig. 6, the large- $x$  effective exponents

$$\beta_q(x, Q^2) = \frac{\partial \ln |q(x, Q^2)|}{\partial \ln(1-x)} \quad (8)$$

are plotted as a function of  $x$  at  $Q^2 = 4 \text{ GeV}^2$  for unpolarized and polarized PDFs,  $q = u, \bar{u}, d, \bar{d}, \bar{s}, g$  and  $q = \Delta u, \Delta \bar{u}, \Delta d, \Delta \bar{d}, \Delta \bar{s}, \Delta g$ . The corresponding values at  $x = 0.9$  are reported in Tab. 3.

The NNPf expectations, displayed in Tabs. 2-3 and in Figs. 2, 4-6, are obtained using polarized NNPf<sub>pol1.1</sub> [16] and unpolarized NNPf2.3 [20] parton sets at NLO accuracy. All uncertainties are nominal one- $\sigma$  bands. The neutron and proton spin-dependent virtual photoabsorption asymmetries,  $A_1^p$  and  $A_1^n$  in Tab. 2 and Fig. 5, are computed from the corresponding polarized and unpolarized structure functions  $g_1, g_2$  and  $F_1$ , by inversion of *e.g.* Eq. (18) in Ref. [12]. Nucleon mass effects are taken into account in the relation between asymmetries and structure functions, consistently with the way kinematic higher-twist terms, *i.e.* target mass corrections, were included in

the relation between structure functions and PDFs when the latter were originally fitted to data [12]. Specifically, the twist-two contribution to the  $g_2$  structure function is related to  $g_1$  via Wandzura-Wilczek relation [57], and zero twist-three contribution to  $g_2$  is assumed. Dynamic higher-twist contributions to the structure functions  $g_1$  and  $g_2$  from Wilson expansion are systematically neglected for consistency with Refs. [12, 16]. Indeed, these were shown to be negligible in Ref. [12], though not in the large- $x$  and small- $Q^2$  kinematic region (see also the discussion at the end of this section).

No model assumptions were imposed for the large- $x$  behavior of PDFs in all NNPf fits, except mutually consistent constraints from positivity of cross sections. In particular, the LO positivity bound was used in the polarized case, see Eqs. (60)-(61) in Ref. [12] and discussion therein.

Inspection of Tab. 2 and Figs. 2, 4-6 allows for drawing the following conclusions.

- A comparison between NNPf predictions and model expectations for PDF ratios and asymmetries allows for testing the validity of each model. It follows that some of them are disfavored. Specifically, the QHD model, with the two different SU(6)-breaking mechanisms considered here [48], systematically overestimates the NNPf result. The statistical model [42]

Model	Refs.	$d/u$	$\Delta d/\Delta u$	$\Delta u/u$	$\Delta d/d$	$A_1^n$	$A_1^p$
SU(6)	[45]	1/2	-1/4	2/3	-1/3	0	5/9
RCQM	[47]	0	0	1	-1/3	1	1
QHD ( $\sigma_{1/2}$ )	[48]	1/5	1/5	1	1	1	1
QHD ( $\psi_\rho$ )	[48]	0	0	1	-1/3	1	1
NJL	[49]	0.20	-0.06	0.80	-0.25	0.35	0.77
DSE ( <i>realistic</i> )	[50]	0.28	-0.11	0.65	-0.26	0.17	0.59
DSE ( <i>contact</i> )	[50]	0.18	-0.07	0.88	-0.33	0.34	0.88
pQCD	[54]	1/5	1/5	1	1	1	1
NNPDF ( $x = 0.7$ )	[16, 20]	$0.22 \pm 0.04$	$-0.07 \pm 0.12$	$0.07 \pm 0.05$	$-0.19 \pm 0.34$	$0.41 \pm 0.31$	$0.75 \pm 0.07$
NNPDF ( $x = 0.8$ )	[16, 20]	$0.18 \pm 0.09$	$0.12 \pm 0.23$	$0.70 \pm 0.13$	$0.34 \pm 0.67$	$0.57 \pm 0.61$	$0.75 \pm 0.12$
NNPDF ( $x = 0.9$ )	[16, 20]	$0.06 \pm 0.49$	$0.51 \pm 0.69$	$0.61 \pm 0.48$	$0.85 \pm 6.55$	$0.36 \pm 0.61$	$0.74 \pm 0.34$

Table 2: A collection of several model expectations for various ratios of polarized/unpolarized PDFs and spin-dependent neutron and proton asymmetries,  $A_1^n$  and  $A_1^p$ , at  $x \rightarrow 0$ . The NNPDF prediction, obtained using unpolarized NNPDF2.3 [20] and polarized NNPDFpol1.1 [16] parton sets, is shown at  $Q^2 = 4 \text{ GeV}^2$  for different values of  $x$ .

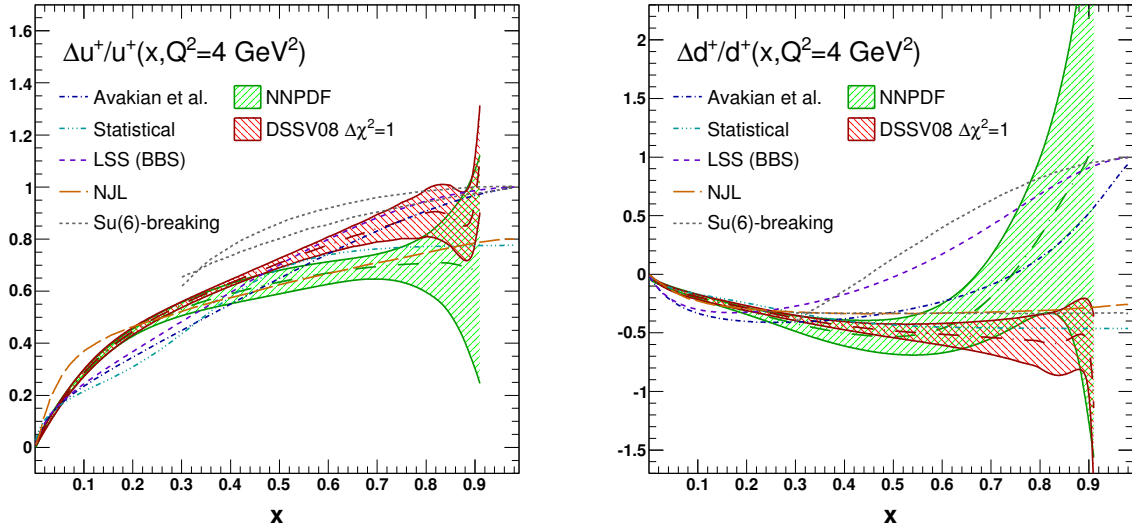


Figure 4: The ratio of polarized to unpolarized total  $u$  (left) and  $d$  (right) quark combinations as a function of  $x$ . Predictions obtained with NNPDF and DSSV08 parton sets are compared with expectations provided by various theoretical models, see the text for details. All results are displayed at  $Q^2 = 4 \text{ GeV}^2$ .

fails in the description of the ratio of polarized to unpolarized PDFs: indeed, it assumes zero gluon polarization at the initial input scale  $Q^2 = 4 \text{ GeV}^2$ , while recent jet production data in polarized  $pp$  collisions at RHIC [58] have definitely pointed towards a positive gluon polarization [15, 16]<sup>2</sup>. The RCQM [47] slightly overestimates the NNPDF result for the neutron photoabsorption asymmetry  $A_1^n$  in the  $x$  region covered by experimental data, with which the NNPDF result is in good agreement. A substantial discrepancy is also seen between the LSS(BBS) [43] and the NNPDF predictions, the former always being larger than the latter. A reasonable agreement

is finally found between NNPDF and both the NJL model [49] and the parameterization by Avakian *et al.* [55], which explicitly included subleading terms of the form  $\ln^2(1-x)$  in the PDF parameterization.

- The comparison between predictions obtained from global QCD analyses, namely NNPDF and DSSV08, is interesting in two respects. Concerning the ratio of polarized to unpolarized total  $u$  and  $d$  quark combinations, the two parton sets are in perfect agreement at  $x \lesssim 0.3$ , while they are slightly different at  $x \gtrsim 0.3$ . Interestingly, for  $d$  quarks, the NNPDF prediction turns up to positive values around  $x = 0.75$ , while the DSSV08 prediction remains negative. Concerning the ratio of polarized to unpolarized gluon, the NNPDF prediction is larger than the DSSV08 prediction. This is due to the different behavior of the polarized gluon in the two parton sets: indeed, this

<sup>2</sup>The original analysis in Ref. [42] has been recently revised [59], allowing for a nonzero gluon polarization at the initial input scale. A large gluon polarization, comparable with that of Refs. [15, 16], is found in Ref. [59].

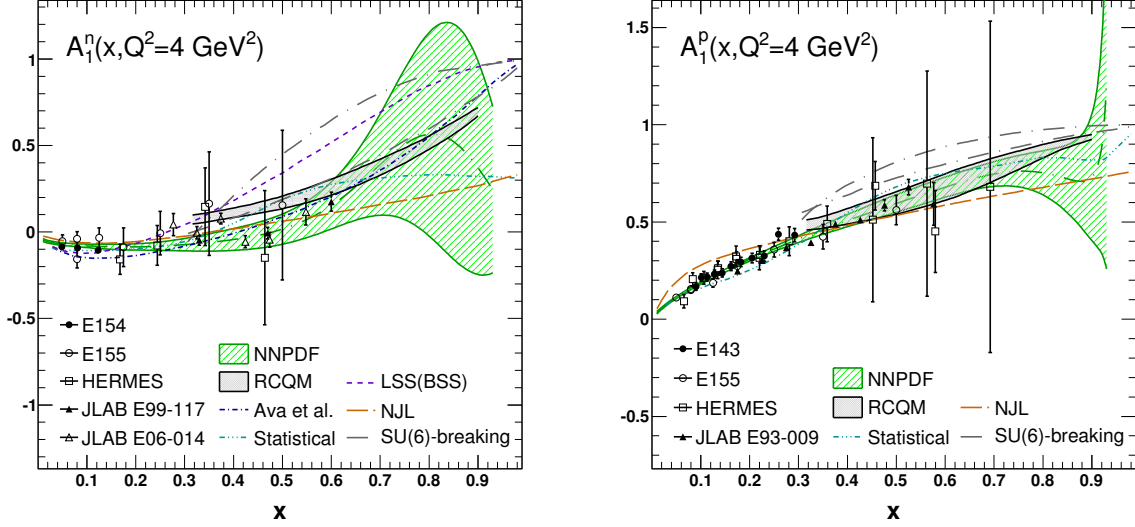


Figure 5: The neutron (left) and proton (right) spin-dependent virtual photoabsorption asymmetry,  $A_1^n$  and  $A_1^p$ , as a function of  $x$ . Predictions obtained with NNPf parton sets are compared with expectations provided by various theoretical models and with available experimental data, see the text for details. All results are displayed at  $Q^2 = 4 \text{ GeV}^2$ .

PDF set	Ref.	$u$	$\bar{u}$	$d$	$\bar{d}$	$\bar{s}$	$g$
NNPDF2.3	[20]	$3.23 \pm 0.21$	$2.09 \pm 1.07$	$2.20 \pm 1.46$	$2.09 \pm 1.07$	$2.95 \pm 0.74$	$3.82 \pm 0.37$
NNPDFp11.1	[16]	$3.08 \pm 0.64$	$1.65 \pm 0.55$	$1.69 \pm 0.99$	$1.89 \pm 0.66$	$1.95 \pm 0.63$	$3.64 \pm 0.47$

Table 3: The values of large- $x$  effective exponents, Eq. (8), at  $x = 0.9$  and  $Q^2 = 4 \text{ GeV}^2$ .

is definitely positive in NNPfpo11.1, while it has a node in DSSV08. The reason for this difference is that jet production data in polarized  $pp$  collisions were included in NNPfpo11.1, but were not in the original DSSV08 analysis. Actually, the latter has been recently updated [15] with the inclusion of these data, and a gluon polarization comparable to that in NNPfpo11.1 was found.

- The possibility to discriminate between models at very large- $x$  values is limited by the wide uncertainties which affect the NNPf predictions. Indeed, all model expectations at  $x \rightarrow 1$  provided in Tab. 2 are compatible, within uncertainties, with the NNPf result at  $x = 0.9$  and  $x = 0.8$ . At a more moderate value of  $x$ ,  $x = 0.7$ , uncertainties are well under control. This suggest that the behavior of PDFs remains largely uncertain at  $x \gtrsim 0.7$ , where no experimental data are available. Furthermore, as the endpoint  $x = 1$  is approached, the accuracy of NLO perturbative evolution is affected by powers of  $\ln(1-x)$  which appear in the perturbative coefficients. Also nonperturbative effects, like instantons or axial ghosts, may become relevant (see *e.g.* Sec. 9 of Ref. [60]).
- The effective exponents  $\beta_q$ , defined by Eq. (8), estimate the powerlike behavior of PDFs at sufficiently large  $x$  values, where the latter can be approximated

as  $q \sim (1-x)^{\beta_q}$ ;  $q$  denotes either unpolarized or polarized distributions, respectively  $q = u, \bar{u}, d, \bar{d}, \bar{s}, g$  or  $q = \Delta u, \Delta \bar{u}, \Delta d, \Delta \bar{d}, \Delta \bar{s}, \Delta g$ . Results in Tab. 3 and in Fig. 6 suggest that the behavior of effective exponents for quark and antiquarks distributions is consistent, within uncertainties, with the expectation based on QCD counting rules [54, 61]. Indeed, these predict that, for a nucleon with helicity  $+1/2$ ,

$$q \xrightarrow{x \sim 1} (1-x)^{2n_s-1} + (1-x)^{2n_s+1}, \quad (9)$$

$$\Delta q \xrightarrow{x \sim 1} (1-x)^{2n_s-1} - (1-x)^{2n_s+1}, \quad (10)$$

with  $n_s$  the number of spectator quarks. Assuming  $n_s = 2$ , it follows that the leading behavior of both unpolarized and polarized PDFs is  $q \sim \Delta q \sim (1-x)^3$  as  $x \rightarrow 1$ . However, this behavior cannot hold at all  $Q^2$ , since evolution causes the power of  $(1-x)$  to grow like  $\ln^2 Q^2$  as  $Q^2$  increases: this may explain the deviation from  $\beta_q = 3$  observed in Tab. 3 and Fig. 6.

- At sufficiently large- $x$  values, the effective exponents for both unpolarized and polarized PDFs tend to coincide, and this means that the LO positivity bound  $|\Delta q| \leq q$ ,  $q = u, \bar{u}, d, \bar{d}, \bar{s}, g$  is saturated. Such a behavior occurs at very large values of  $x$ , typically  $x \sim 0.85$ .

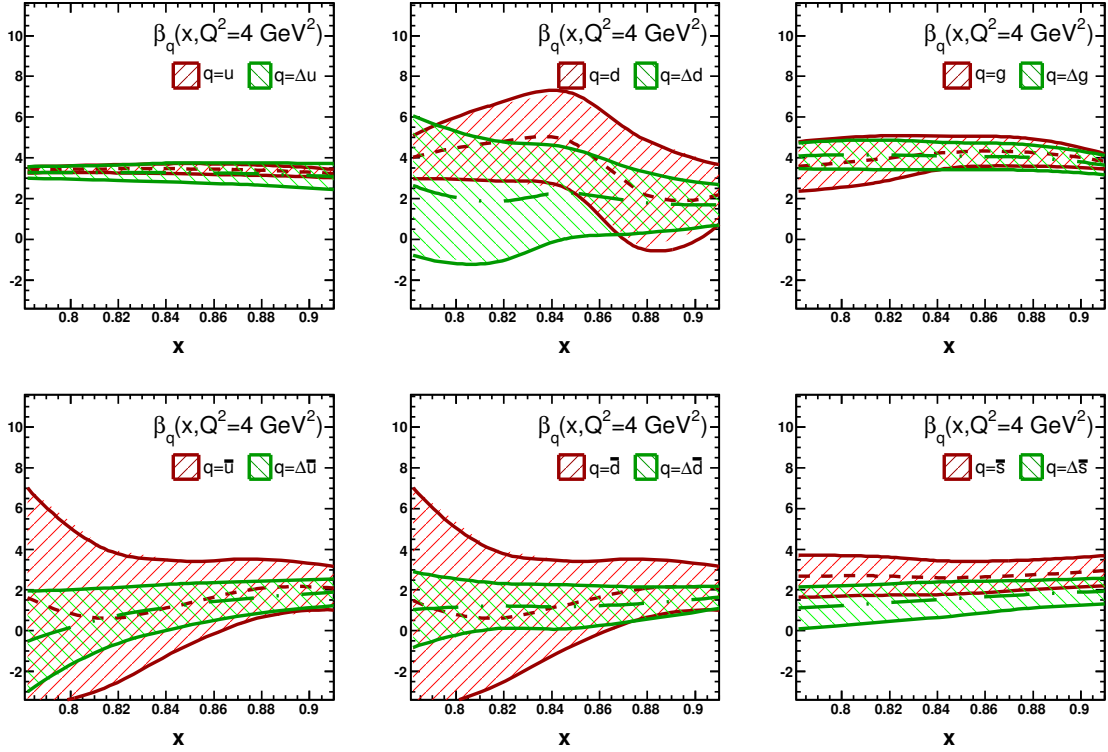


Figure 6: Large- $x$  effective exponents, Eq. (8), at  $Q^2 = 4 \text{ GeV}^2$  as a function of  $x$ .

- A new determination of unpolarized PDFs based on the NNPDF methodology, NNPDF3.0 [62], has been released recently. As in all NNPDF determinations, the neural network parameterization of each PDF  $i$  is supplemented by a preprocessing term of the form  $x^{-a_i}(1-x)^{b_i}$ ;  $a_i$  and  $b_i$  are chosen, at random for each PDF replica, in a given interval of values. In NNPDF2.3, this interval was determined based on a stability analysis of the results, while in NNPDF3.0 and NNPDFpol1.1 this is determined in an automatic and self-consistent way (for details see Ref. [62]). In the future, it would be interesting to study whether the results in Tab. 3 and Fig. 6, including the mutual spreads of the unpolarized and polarized large- $x$  effective exponents, will change upon the methodological improvement introduced in NNPDF3.0.

The investigation of the large- $x$  behavior of polarized PDFs is one of the goals pursued by ongoing and future JLAB experimental programs [19]. Several data sets on neutron and proton asymmetries in inclusive DIS,  $A_1^n$  and  $A_1^p$ , have become available recently, specifically from JLAB E99-117 [63], JLAB E93-009 [64] and JLAB E06-014 [65] experiments. These are shown in Fig. 5, together with E143 [39], E154 [66], E155 [67] and HERMES [41] data sets, but, at variance with the latter, they were not in-

cluded in the NNPDFpol1.1 analysis. A large amount of data on the ratio of polarized to unpolarized proton and deuteron structure functions,  $g_1^{p,d}/F_1^{p,d}$ , has been also measured by CLAS [68] very recently.

Qualitatively, JLAB data appear in agreement with the NNPDF prediction of the neutron and proton photoabsorption asymmetries,  $A_1^n$  and  $A_1^p$ , in Fig. 5. Nevertheless, it is apparent that they are much more accurate than previous measurements already included in NNPDFpol1.1. In order to quantitatively assess the impact of JLAB data on PDFs, one should then include them in a global determination, with a careful treatment of dynamic higher-twist contributions to the Wilson expansion. Indeed, JLAB data are taken in a kinematic region (large  $x$ , small  $Q^2$ ) where the inclusion of these effects were shown to be essential for describing them correctly [14].

In a previous NNPDF analysis [12], a conservative cut on the squared invariant mass of the hadronic final state  $W^2 = m^2 + Q^2(1-x)/x$ , with  $m$  the nucleon target mass, was imposed in order to remove experimental data which may be affected by sizable higher-twist corrections. The cut was set to  $W^2 \geq W_{\text{cut}}^2 = 6.25 \text{ GeV}^2$ , because above this threshold higher-twist contributions become compatible with zero, when added to the observables with a coefficient fitted to the data [69]. Following this choice, almost all JLAB data are excluded, except few points in the

JLAB E06-014 [65] and CLAS [68] sets. For this reason, the inclusion of JLAB data in a determination of polarized PDFs based on the NNPDF methodology is left for future work. Of course, this should include a careful treatment of dynamic higher-twist contributions along the lines of what has already been presented in the unpolarized case [70].

*Conclusions.* I have studied the behavior of polarized parton distributions in the regions of small and large momentum fractions, based on previous mutually consistent NNPDF determinations of polarized [16] and unpolarized [20] PDFs. Among all PDF sets, these are the best suited in order for such a study to be effective: indeed, they include all the relevant experimental information which is presently available, and they are determined with a methodology devised to provide a minimally biased result.

I have investigated the potential of NNPDF parton sets in discriminating the reliability of several theoretical models of polarized nucleon structure, by comparing expectations for relevant observables based on them with the corresponding predictions obtained with NNPDF. Only a limited number of models are clearly disfavored, while the possibility to discriminate between the others is seriously limited by the large uncertainties which affect the NNPDF predictions at both small- and large- $x$  values.

The experimental information which will be provided either by a future high-energy polarized EIC [18] or by 12 GeV JLAB upgrade [19] will significantly reduce PDF uncertainties in global determinations, at small and large  $x$  respectively, and finally improve our knowledge of the nucleon spin structure in these regions.

## Acknowledgements

I would like to thank S. Forte, G. Ridolfi and J. Rojo for their useful comments to the manuscript. I also acknowledge the kind hospitality of the theory group at the Nationaal instituut voor subatomaire fysica (Nikhef), where this work was partly performed. This research was supported by an Italian PRIN2010 grant and by a European Investment Bank EIBURS grant.

## References

- [1] S.D. Bass, *Rev.Mod.Phys.* 77 (2005) 1257, hep-ph/0411005.
- [2] S. Kuhn, J.P. Chen and E. Leader, *Prog.Part.Nucl.Phys.* 63 (2009) 1, 0812.3535.
- [3] J. Bjorken, *Phys.Rev.* 148 (1966) 1467.
- [4] J.R. Ellis and R.L. Jaffe, *Phys.Rev.* D9 (1974) 1444.
- [5] H. Burkhardt and W. Cottingham, *Annals Phys.* 56 (1970) 453.
- [6] A. Efremov, O. Teryaev and E. Leader, *Phys.Rev.* D55 (1997) 4307, hep-ph/9607217.
- [7] N. Cabibbo, E.C. Swallow and R. Winston, *Ann.Rev.Nucl.Part.Sci.* 53 (2003) 39, hep-ph/0307298.
- [8] M. Hirai and S. Kumano, *Nucl.Phys.* B813 (2009) 106, 0808.0413.
- [9] D. de Florian et al., *Phys.Rev.* D80 (2009) 034030, 0904.3821.
- [10] E. Leader, A.V. Sidorov and D.B. Stamenov, *Phys.Rev.* D82 (2010) 114018, 1010.0574.
- [11] J. Blumlein and H. Bottcher, *Nucl.Phys.* B841 (2010) 205, 1005.3113.
- [12] The NNPDF Collaboration, R.D. Ball et al., *Nucl.Phys.* B874 (2013) 36, 1303.7236.
- [13] F. Arbabifar, A.N. Khorramian and M. Soleymaninia, *Phys.Rev.* D89 (2014) 034006, 1311.1830.
- [14] P. Jimenez-Delgado, A. Accardi and W. Melnitchouk, *Phys.Rev.* D89 (2014) 034025, 1310.3734.
- [15] D. de Florian et al., *Phys.Rev.Lett.* 113 (2014) 012001, 1404.4293.
- [16] NNPDF Collaboration, E.R. Nocera et al., *Nucl.Phys.* B887 (2014) 276, 1406.5539.
- [17] E.R. Nocera, (2014), 1403.0440.
- [18] A. Accardi et al., (2012), 1212.1701.
- [19] J. Dudek et al., *Eur.Phys.J.* A48 (2012) 187, 1208.1244.
- [20] The NNPDF Collaboration, R.D. Ball et al., *Nucl.Phys.* B867 (2013) 244, 1207.1303.
- [21] R.D. Ball et al., *JHEP* 1304 (2013) 125, 1211.5142.
- [22] R. Heimann, *Nucl.Phys.* B64 (1973) 429.
- [23] S.D. Bass, *Mod.Phys.Lett.* A22 (2007) 1005, hep-ph/0606067.
- [24] S. Bass and P. Landshoff, *Phys.Lett.* B336 (1994) 537, hep-ph/9406350.
- [25] F. Close and R. Roberts, *Phys.Lett.* B336 (1994) 257, hep-ph/9407204.
- [26] R.D. Ball, S. Forte and G. Ridolfi, *Nucl.Phys.* B444 (1995) 287, hep-ph/9502340, Erratum-ibid. B449 (1995) 680.
- [27] G. Altarelli et al., *Acta Phys.Polon.* B29 (1998) 1145, hep-ph/9803237.
- [28] T. Gehrmann and W.J. Stirling, *Phys.Lett.* B365 (1996) 347, hep-ph/9507332.
- [29] M. Ahmed and G.G. Ross, *Phys.Lett.* B56 (1975) 385.
- [30] J. Bartels, B. Ermolaev and M. Ryskin, *Z.Phys.* C70 (1996) 273, hep-ph/9507271.
- [31] J. Bartels, B. Ermolaev and M. Ryskin, *Z.Phys.* C72 (1996) 627, hep-ph/9603204.
- [32] B. Ermolaev, M. Greco and S. Troyan, *Phys.Lett.* B579 (2004) 321, hep-ph/0307128.
- [33] S. Moch, J. Vermaseren and A. Vogt, (2014), 1409.5131.
- [34] S.J. Brodsky and I. Schmidt, *Phys.Lett.* B234 (1990) 144.
- [35] S.J. Brodsky, M. Burkardt and I. Schmidt, *Nucl.Phys.* B441 (1995) 197, hep-ph/9401328.
- [36] The NNPDF Collaboration, R.D. Ball et al., *Phys.Lett.* B728 (2014) 524, 1310.0461.
- [37] E.C. Aschenauer, R. Sassot and M. Stratmann, *Phys.Rev.* D86 (2012) 054020, 1206.6014.
- [38] Spin Muon Collaboration, B. Adeva et al., *Phys.Rev.* D58 (1998) 112001.
- [39] E143 collaboration, K. Abe et al., *Phys.Rev.* D58 (1998) 112003, hep-ph/9802357.
- [40] COMPASS Collaboration, M. Alekseev et al., *Phys.Lett.* B690 (2010) 466, 1001.4654.
- [41] HERMES Collaboration, A. Airapetian et al., *Phys.Rev.* D75 (2007) 012007, hep-ex/0609039.
- [42] C. Bourrely, J. Soffer and F. Buccella, *Eur.Phys.J.* C23 (2002) 487, hep-ph/0109160.
- [43] E. Leader, A.V. Sidorov and D.B. Stamenov, *Int.J.Mod.Phys.* A13 (1998) 5573, hep-ph/9708335.
- [44] J. Blumlein and A. Vogt, *Phys.Lett.* B386 (1996) 350, hep-ph/9606254.
- [45] F. Close, *Nucl.Phys.* B80 (1974) 269.
- [46] F. Close, *Phys.Lett.* B43 (1973) 422.
- [47] N. Isgur, *Phys.Rev.* D59 (1999) 034013, hep-ph/9809255.
- [48] F. Close and W. Melnitchouk, *Phys.Rev.* C68 (2003) 035210, hep-ph/0302013.
- [49] I. Cloet, W. Bentz and A.W. Thomas, *Phys.Lett.* B621 (2005) 246, hep-ph/0504229.
- [50] C.D. Roberts, R.J. Holt and S.M. Schmidt, *Phys.Lett.* B727 (2013) 249, 1308.1236.
- [51] M. Wakamatsu, (2014), 1405.7095.
- [52] N. Kochelev, *Phys.Rev.* D57 (1998) 5539, hep-ph/9711226.
- [53] C. Boros and A.W. Thomas, *Phys.Rev.* D60 (1999) 074017,

- hep-ph/9902372.
- [54] G.R. Farrar and D.R. Jackson, *Phys.Rev.Lett.* 35 (1975) 1416.
  - [55] H. Avakian et al., *Phys.Rev.Lett.* 99 (2007) 082001, 0705.1553.
  - [56] A. Martin et al., *Eur.Phys.J. C* 28 (2003) 455, hep-ph/0211080.
  - [57] S. Wandzura and F. Wilczek, *Phys.Lett. B* 72 (1977) 195.
  - [58] STAR Collaboration, L. Adamczyk et al., (2014), 1405.5134.
  - [59] C. Bourrely and J. Soffer, (2014), 1408.7057.
  - [60] M. Anselmino, A. Efremov and E. Leader, *Phys.Rept.* 261 (1995) 1, hep-ph/9501369, Erratum-ibid. 281 (1997) 399-400.
  - [61] S.J. Brodsky and G.P. Lepage, *Phys.Scripta* 23 (1981) 945.
  - [62] The NNPDF Collaboration, R.D. Ball et al., (2014), 1410.8849.
  - [63] JLab Hall A Collaboration, X. Zheng et al., *Phys.Rev. C* 70 (2004) 065207, nucl-ex/0405006.
  - [64] CLAS Collaboration, K. Dharmawardane et al., *Phys.Lett. B* 641 (2006) 11, nucl-ex/0605028.
  - [65] Jefferson Lab Hall A Collaboration, D. Parno et al., (2014), 1406.1207.
  - [66] E154 Collaboration, K. Abe et al., *Phys.Rev.Lett.* 79 (1997) 26, hep-ex/9705012.
  - [67] E155 Collaboration, P. Anthony et al., *Phys.Lett. B* 493 (2000) 19, hep-ph/0007248.
  - [68] CLAS Collaboration, Y. Prok et al., *Phys.Rev. C* 90 (2014) 025212, 1404.6231.
  - [69] C. Simolo, (2006), 0807.1501.
  - [70] The NNPDF Collaboration, R.D. Ball et al., *Phys.Lett. B* 723 (2013) 330, 1303.1189.